

**ASPECTS OF  $R_g$  AND  $L_g$  GENERATION FROM THE SHAGAN DEPTH OF BURIAL EXPLOSIONS**

Jessie L. Bonner,<sup>1</sup> Howard J. Patton,<sup>2</sup> Anca C. Rosca,<sup>1</sup> Heather Hooper,<sup>1</sup> Jeffrey Orrey,<sup>3</sup>  
Mark Leidig,<sup>1</sup> and Indra Gupta<sup>4</sup>

Weston Geophysical Corporation,<sup>1</sup> Los Alamos National Laboratory; <sup>2</sup> GeoVisual Tech; <sup>3</sup> and Multimax, Inc. <sup>4</sup>

Sponsored by National Nuclear Security Administration  
Office of Nonproliferation Research and Engineering  
Office of Defense Nuclear Nonproliferation

Contract No. DE-FG02-00ER83123

**ABSTRACT**

Regional  $S$ -wave amplitudes observed on recordings from the Depth of Burial (DOB) experiments conducted at the Shagan Test Site in August and September 1997 varied according to source depth (Phillips *et al.*, 1998; Myers *et al.*, 1999). Similar depth dependence was noted on nearfield recordings of  $R_g$  waves. These are significant observations in support of nearfield  $R_g$ -to- $S$  scattering proposed by Gupta and co-workers in the early 90s (Gupta *et al.*, 1992). Unfortunately, the importance of nearfield scattering relative to competing mechanisms of  $S$ -wave generation by underground explosions remains unresolved in part due to the need for a phenomenological model with which to predict  $S$ -wave amplitudes and their yield scaling as a function of source and material parameters. One of the goals of this project is to begin developing such a model by describing source mechanisms of  $R_g$  excitation using simple elastodynamic models for explosion sources, and by examining the effects of different source depths on  $P$ -to- $S$  conversions at the free surface using two- and three- dimensional Generalized Fourier Methods.

Very little is known about  $R_g$  excitation by underground explosions. To fit observations of  $L_g$  spectral ratios, Patton and Taylor (1995) invoke  $R_g$ -to- $S$  scattering and a linear superposition of spatially distributed sources to excite  $R_g$  waves: a pure point-source explosion (monopole) and a compensated linear vector dipole (CLVD) with shallower depth compared to the DOB. The CLVD source is believed to be associated with large deformations over the detonation point related to spallation, block motions, and dynamic rebound caused by the outgoing shock wave. This compound source model will be tested against nearfield and farfield recordings of the DOB chemical explosions. We extracted  $R_g$  waves from nearfield records and carried out spectral analysis to recover source amplitudes and phase. Significant differences between the recovered source spectra and spectra predicted for a monopole source suggest that the source of  $R_g$  waves for all three DOB explosions depart significantly from a pure point-source explosion. Modeling will be performed to investigate whether the addition of a CLVD source can explain the observations. Furthermore, comparisons between the absolute amplitudes predicted by source models and those observed for regional  $S$  waves will help characterize the scattering transfer function and the energetics of mode conversion.

We have completed a series of GFM2D simulations in order to examine  $S$ -waves generated from free surface reflections. We generated a model consisting of the shallow structure of the Shagan Test Site determined from  $R_g$  inversions overlying the eastern Kazakhstan model of Priestley *et al.* (1988). For this model, significant shear wave energy can be trapped in the crust from explosions at 300 and 550 m depth to form a regional  $L_g$  phase. Comparison of the synthetics to regional data shows that the different depths of burial for the two sources can account for much of the observed differences in 0.7-3 Hz  $L_g$  amplitudes at MAK. Additional models with random velocity heterogeneities and laterally varying structure are also being examined to further quantify the regional observations.

## **OBJECTIVES**

The objectives of this research project are to create physically realistic models of short-period (0.2 to 12 seconds) surface wave generation from earthquakes, small chemical explosions and different classifications of mine blasts, and to understand the propagation characteristics of these surface waves, including mechanisms for explosion-generated  $Lg$ . To accomplish these objectives, we have:

- Examined whether a pure point-source explosion (monopole) and a compensated linear vector dipole (CLVD) with shallow depth can explain the  $Rg$  recorded at the Shagan Depth of Burial (DOB) experiments,
- Continued development of a numerical modeling package to generate short-period surface waves from different explosion sources and to propagate them through complex 3D and 2D media, and
- Compared preliminary numerical results to empirical data to aid in development of regional explosion discriminants based upon surface waves.

The preliminary results of modeling DOB  $Rg$  source spectra with the CLVD source, updates to the development of the 3D and 2D surface wave modeling program, and applications of the modeling package are presented in the following paper.

## **RESEARCH ACCOMPLISHED**

### **CLVD Modeling for the Shagan DOB Explosions (Patton, Gupta, and Bonner)**

**Introduction.** Local and regional seismic recordings of three 25-ton chemical explosions comprising the DOB experiment at the Shagan Test Site (Myers *et al.*, 1999; Bonner *et al.*, 2001) offer a unique opportunity to investigate the excitation of near-field, short-period, fundamental-mode surface waves ( $Rg$ ) and the relationships these  $Rg$  waves have with waves recorded at greater distances. Interest in these relationships has grown steadily in recent years as evidence accumulates that  $Rg$ -to- $S$  scattering is an important mechanism for the generation of regional  $S$  waves by underground explosions. Due to the importance of  $Lg$  and  $Lg$  coda waves for discrimination and yield estimation, it is crucial that a physical model for the genesis of regional  $S$  waves is well understood for underground explosions. Unfortunately, there is much controversy over the causes of  $S$ -wave generation by explosions, and much of the evidence gathered to date in support of  $Rg$ -to- $S$  scattering is only qualitative in nature. A physical model will be advanced significantly if observations relevant to  $Rg$ -to- $S$  scattering can be put on firm quantitative footing.

Very little is known about the excitation of  $Rg$  waves by underground explosions. It has long been recognized that shallow sources in the Earth should excite  $Rg$  waves efficiently. However, the excitation of  $Rg$  waves by explosions may be very complex because real world explosions are usually not simple monopole (point isotropic) sources, but rather complex, anisotropic sources distributed in time and space. One model for the excitation of  $Rg$  waves invokes a compensated linear vector dipole (CLVD) to explain the frequency content of  $Lg$  spectra and spectral ratio observations for nuclear explosions (Patton and Taylor, 1995; Gupta *et al.*, 1997). In this case, the CLVD is an elastodynamic equivalent of a conical source, with apex at the detonation point, extending to the free surface, and the material within the volume undergoes catastrophic shear failure. This source is believed to be associated with large deformations accompanying underground explosions in the form of spallation, tensile failures and block motions below the spalled layers, as well as dynamic rebound caused by the outgoing shock wave.

The objective of this study is to characterize  $Rg$  waves recorded within 20 km of three chemical explosions, all with the same yield, but buried at significantly different depths. Scaled depth of burials (sDOB) for these explosions span a wide range, and source phenomenologies accompanying these explosions are expected to exhibit great variability. Indeed, the shallowest explosion is known to have cratered, while the deepest explosion, with sDOB of  $\sim 1400$  scale meters, was significantly over buried. Theoretically, the more over buried an explosion is, the more like a monopole it should behave. The spectral amplitude and the phase of  $Rg$  waves from the DOB explosions have been studied in light of the variant phenomenology, and source models are proposed to explain the observed source spectra. In particular, the CLVD source model has been tested. The preliminary results are presented in this paper.

**New Velocity Models.** Bonner *et al.* (2001) presented averaged velocity structures for the upper 2.5 km at the Shagan Test Site (STS) for both the northeastern and southwestern sections. The structures were obtained by inversion of group velocity dispersion curves obtained from local recordings of the DOB experiment. For the present study, we conducted a new set of inversions for paths either completely or partially within the southwestern section of STS. The objective of the current study was to obtain additional information about the upper crust at depths deeper than 2.5 km (in some cases as deep as 10 km). The starting model for these inversions consisted of a combination of the averaged model for the southwestern test site (Bonner *et al.*, 2001 Figure 11) and the Priestley *et al.* (1988) model for Eastern Kazakhstan (EK). For some paths, two-station phase velocity data at short periods were used to further constrain the inversions. We then performed least-squares inversions on both the phase and group velocity dispersion curves. The inversion resulted in a new set of models, called Shagan+EK, for each DOB source-station path of interest.

**Processing.** The first processing step completed was to identify  $R_g$  on the local seismic recordings of the DOB experiments. We used particle motion and arrival times predicted from the new velocity models to identify  $R_g$  on the waveforms. We found that particle motions were quite troublesome for certain stations, while they were generally well-behaved for others. The troublesome stations were S4, S6, and S9, all of which have paths for the three DOB shots that tend to cut across the grain of the “geologic fabric” more so than do the paths for S2, S3, S7, and S8. Waveforms also tend to be more complex for S4, S6, and S9, which is probably caused by signal-generated noise due to inhomogeneities along the path. We are also examining the possibility that there may be instrument problems at these stations (in fact, we are verifying the responses for all local stations), thus the results presented in this paper are focused on stations S2, S3, S7, and S8. Further processing steps included multiple-filter analyses and time variable filtering to extract the  $R_g$  from the complex seismograms.

**Spectral Analyses.** We completed spectral analyses of the signals and compared them with synthetic signals generated for a monopole explosion. Figure 1 summarizes  $R_g$  spectral amplitude and phase observations for the three DOB shots. Attenuation-corrected, weighted mean amplitude spectra are shown with their model spectra in the top panels of Figure 1. Note that the mean spectra were determined using stations S2, S3, S7, and S8 for the 50 m and 300 m shots, while the mean spectra for the 550 m shot are based on only S3, S7, and S8 since S2 was too close to the source. The  $M_0$  used for the model spectrum of the 50 m shot,  $2.8 \times 10^{13}$  Nm, was determined from Denny and Johnson’s (1991) scaling relationships. Likewise, the  $M_0$  for the 300 m and 550 m explosions were determined to be  $1.2 \times 10^{13}$  Nm and  $1.0 \times 10^{13}$  Nm, respectively. Mean phase spectra are plotted on the bottom row of Figure 1, where the units are circles. Discontinuities in the observations for the 550 m explosion are caused by phase wraparound.

The observed  $R_g$  phase spectra results are very interesting in light of their associated amplitude spectra and model spectra. Both amplitudes and phases indicate that the simplest model of an explosion source, the pure monopole, is inadequate to explain the frequency content of nearfield  $R_g$  signals for all three explosions. Considering the sDOB of the 550 m explosion (~1400), this finding is remarkable. On the other hand, the ground-zero accelerometer record for this shot does show evidence of spall, so from a phenomenological standpoint, even this shot was probably not a point dilatational source. While the final phase spectrum for the 550 m explosion (solid line in third frame on the bottom) is somewhat noisy, it nevertheless shows different behavior compared to spectra from the other explosions. Likewise, there are differences in the spectral shapes of observed amplitude.

**CLVD Source.** CLVD models are a primary focus of this study and have been tested against the spectral observations, both amplitude and phase. The CLVD source,  $M_{xx} = \square 0.5$ ,  $M_{yy} = \square 0.5$ ,  $M_{zz} = 1.0$ ,  $M_{ij} = 0$  for  $i$  not equal to  $j$ , has a vertical axis of symmetry (extension). This source excites azimuthally-independent Rayleigh waves, and does not excite Love waves. Several interesting features characterize the theoretical Rayleigh-wave radiation from such a source, including excitation nulls (Figure 2), which occur in the frequency range of  $R_g$  waves for source depths in the upper 300 m of the crust. The precise location of these nulls depends on the velocity structure as well as source depth. We used the Shagan+EK model to generate the CLVD source amplitude spectra in Figure 2.

Another interesting feature of the CLVD radiation is the source phase. For frequencies below the null frequency, the source phase is -0.125 circles, and above the null frequency, it’s 0.375 circles. This assumes a step function time history. Thus if a point CLVD source at 50 m depth is coincident in time and space (epicenter) with a pure monopole source, Rayleigh waves will experience destructive interference below 5 Hz and constructive interference above 5 Hz since the waves excited by the CLVD and monopole sources are perfectly out of phase and in phase on

either side of the null frequency. The source phase characteristics of these sources lead to very interesting interference patterns which show additional complexity as more realism is introduced into the source. For example, the origin of the CLVD should be time delayed relative to the origin of the monopole. We are attempting to model the nearfield  $R_g$  spectra using a compound source model composed of a linear superposition of monopole and CLVD sources.

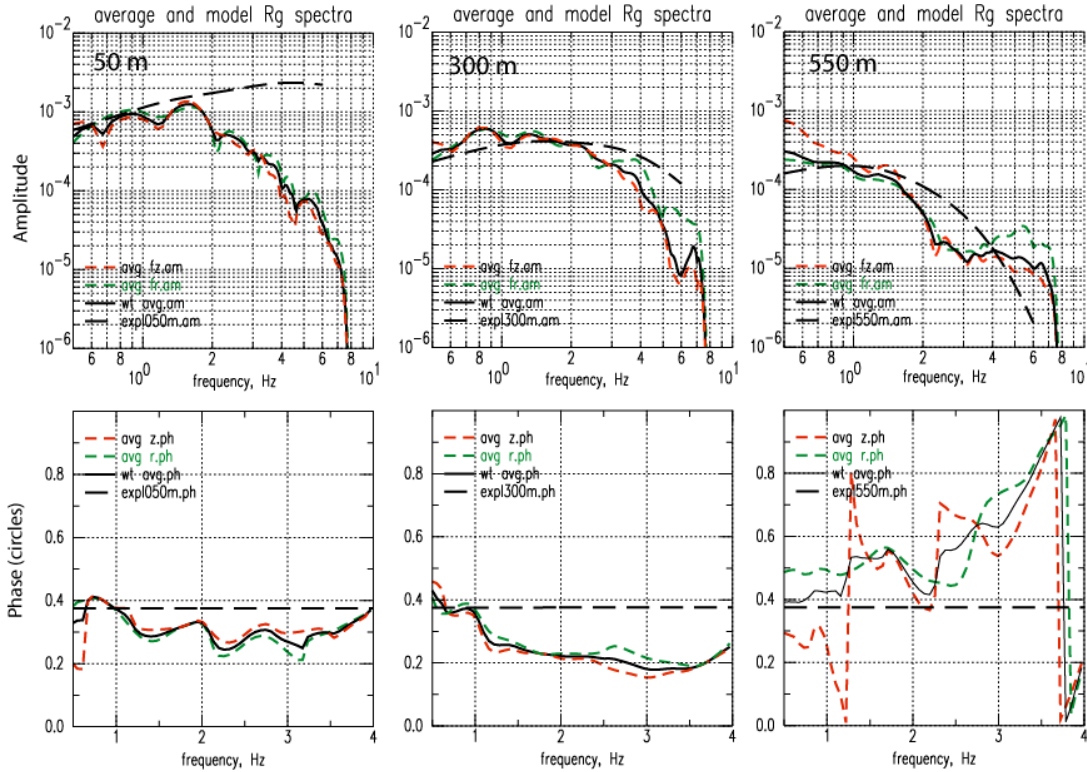


Figure 1. (Top) Amplitude  $R_g$  spectra for the sDOB explosions including the average vertical components (red dashed); averaged radial components (green dashed); the weighted average spectra (solid black); and the spectra for the pure monopole explosions (black dashed line). (Bottom) Phase spectra.

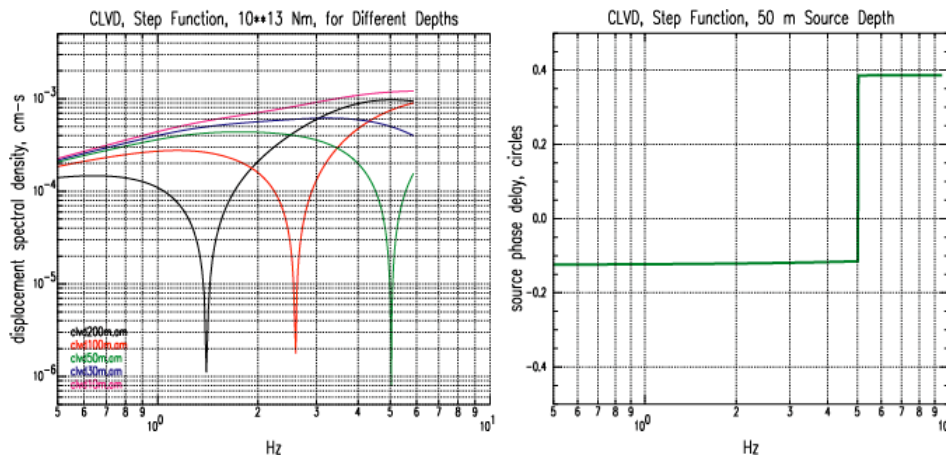


Figure 2. (Left) Theoretical  $R_g$  spectra for a CLVD source at depths of 200 m (black), 100 m (red), 50 m (green), 30 m (blue), and 10 m (magenta). Nulls in the amplitude spectra depend on source depth.  $R_g$  waves below the null frequency are exactly 180 degrees out of phase with  $R_g$  waves from a simultaneous, co-located monopole source with the same time history as the CLVD. Above the null frequency, they are in phase. (Right) A phase spectrum for 50 m depth is plotted in units of circles.

**Advancements in 2D and 3D Modeling of  $R_g$  and  $L_g$  Using GFM (Bonner, Rosca, Orrey, Hooper, and Leidig)**

**Program Enhancements.** We continue to improve the three-dimensional (3D) Generalized Fourier Method (GFM) developed by Orrey *et al.* (2003). GFM3D is a generalization of the standard Fourier pseudospectral method, in which the spatial approximations of the field variables are truncated Fourier series. During the past year, the GFM3D software package has been ported to a cluster of Linux workstations and tested for solution accuracy, reliability and optimal performance. The principal tasks involved in the porting phase have been 1) conversion of the software package’s source code to a cross-platform version to incorporate the specifics of the Linux-based system compilers, 2) debugging of the new version to resolve differences in the MPI implementation on the Linux versus Cray architectures, 3) testing of the compiled system for a set of standard test problems, and 4) optimization of the code performance for the (currently) 9-node cluster. In addition, the code has been enhanced to work in 2D, and we have implemented the capability to convolve different source functions with the synthetics.

The final phase of the code implementation will involve addition of features to increase the range of geophysical problems that can be handled by the code. This includes a general Greens function convolution with different source functions and a non-uniform grid via a coordinate transformation from regular Cartesian coordinates. In addition, tests have indicated a problem with the implementation of anelasticity via the use of memory variables. The code will be completed by November 2003. Additional packages that have been developed for the software include a module that generates 2D profiles from the CRUST2 model (Bassin *et al.*, 2000) and a *gfm2sac* conversion software.

**GFM3D Modeling of the  $L_g$  and  $R_g$  Propagation in Pakistan.** We completed a study to examine whether a GFM3D simulation for station NIL using the 3D CRUST2 model could be used to estimate  $L_g$  and  $R_g$  travel times for velocity model validation. We parameterized the model using a 5 km Cartesian grid spacing out to at least 1000 km in all directions from NIL and to a depth of 200 km. The resulting number of nodes for this simulation was 7.9 million and the time to simulate 400 seconds of data was 47 hours running on a nine-node parallel Linux cluster. We placed a point source at the NIL grid node and calculated full waveform synthetics for every other grid node. Two images of the surface velocities (bandpass filtered between 0.1 and 0.5 Hz) recorded 70 and 191 seconds after the initiation of the simulations are shown in Figure 3. Even though this is a point source simulating an explosion, there is abundant  $S$ -wave energy created by scattering processes within the 3D model. In addition, there is  $L_g$  energy propagating with significant spatial variations in group velocities (ranging between 3.2 and 3.7 km/sec) and amplitudes.

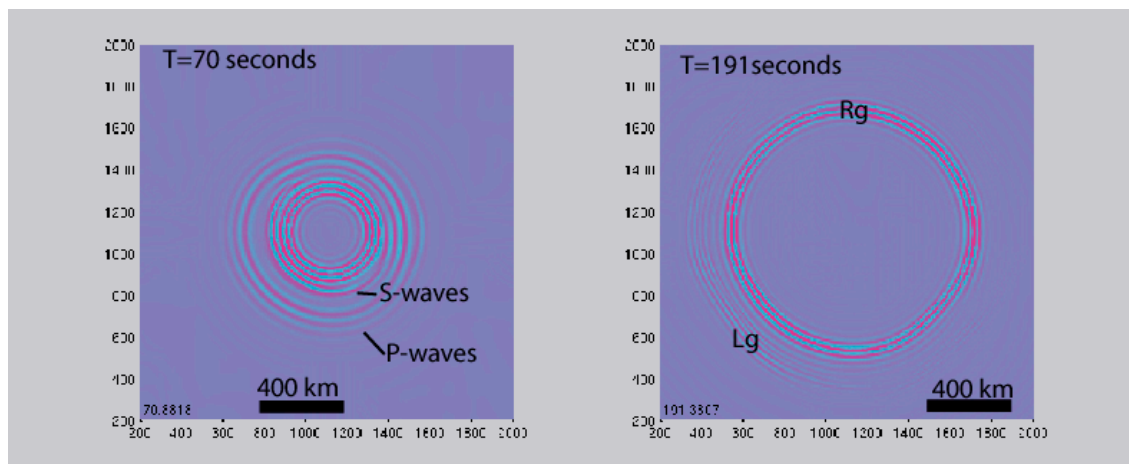


**Figure 3. GFM3D snapshots of synthetic propagation at near-regional distances from station NIL using CRUST2 as the velocity model. The snapshots are of bandpass filtered data (0.1 to 0.5 Hz) at 70 and 191 seconds after initiation of a point source.**

The next stage of the pilot study was to process each synthetic for an  $L_g$  arrival time. Given that there were over 33,000 stations for this simulation, we developed an automated algorithm that normalized the data to the maximum amplitude of the  $L_g$  data within a group velocity window between 3.2 and 4.0 km/sec. The algorithm then applied a

threshold detector within this window of synthetic data and determined the arrival time in which the amplitudes of the  $Lg$  reached 30% of the maximum amplitude in the window. We then divided this arrival time into the epicentral distance to get a node group velocity. The resulting image and randomly-picked synthetic seismograms at various locations within the model are shown in Figure 4. This is, to our knowledge, one of the first images of  $Lg$  group velocities synthesized from 3D full waveform modeling ever produced. We note slower  $Lg$  group velocities in the Katawaz, Tadjik, Tarim, and Indo-Gangetic basins and faster propagation in the Indian shield and other regions. We have completed similar maps for the  $Rg$  phase and intermediate-period Rayleigh waves and are in the process of using the 3D maps to validate the CRUST2 model in this region. We are also doing the same for the Weston Geophysical India and Pakistan 3D model (WINPAK3D).

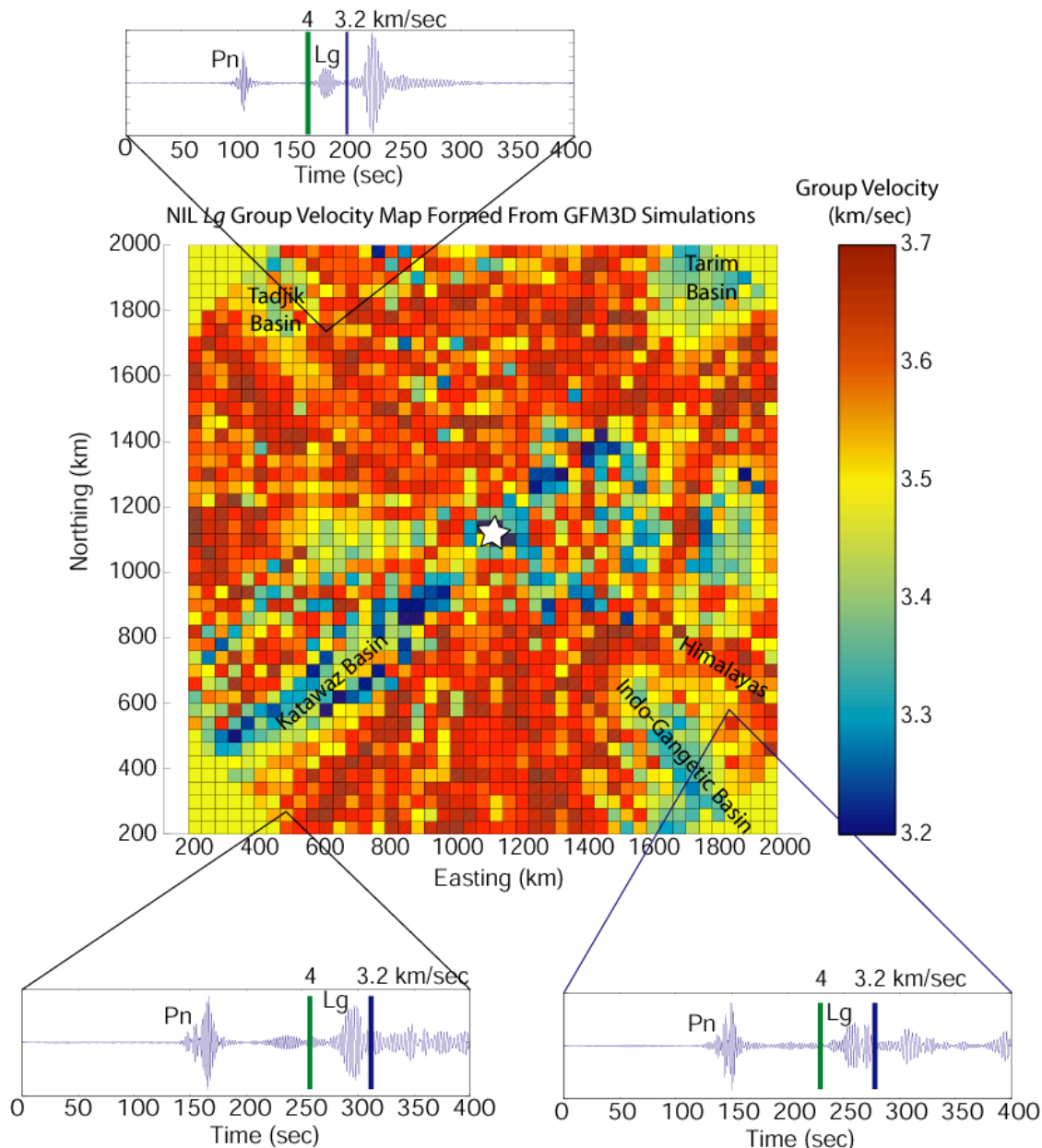


**Figure 4.** Results of  $Lg$  group velocity estimation from GFM3D synthetics for NIL. Example synthetics are shown for three randomly picked stations in the model. A group velocity window between 4 and 3.2 km/sec is shown. The  $Lg$  onset ranges from impulsive to emergent, which is similar to the phase as observed on regional seismograms.

**GFM2D Modeling of the Effects of Basins on  $Lg$  and  $Rg$  Generation from Explosions.** To study the effect of different tectonic features on the generation and propagation of surface waves and  $Lg$ , we generated synthetic waveforms using GFM2D for a range of models and source depths. For this component of the study, we used the EK model in which we embedded various elements such as basins, a rift and a crustal root. Some models included a thin low velocity layer at the top, with the  $P$ -wave velocity lower than the upper mantle  $S$ -wave velocity (termed Ekl). The simulations were performed in a 600x200 km 2D grid with 0.5 km node spacing. The parameters chosen for the basin were calculated as weighted averages of the parameters for soft and hard sediments in CRUST2. Using 20% soft sediments and 80% hard sediments,  $P$  velocity,  $S$  velocity and density are 3.7 km/s, 1.92 km/s and 2.34 g/cm<sup>3</sup> respectively. The same parameters were used for the uppermost low velocity layer when the feature was integrated in the model. Variations in Moho depth (referred to as “root” and “rift”) were generated by lowering or raising the bottom two boundaries of the EK model crust. Each of the embedded structures extends 5 km in the z direction and 100 km laterally. The boundary of the first basin is at 10 km from the edge of the model and the sources were placed at 30 km from the model end. We performed simulations for sources placed within the basin at 1 and 2.5 km depth and below the basin at 5.5 km depth. All waveforms shown in this section were band-pass filtered between 0.001 and 1.0 Hz in order to avoid numerical artifacts for the synthetics. The effects of source depth, the presence of low velocity basins in the source region, and Moho depth variations are discussed below and shown in Figures 5 and 6.

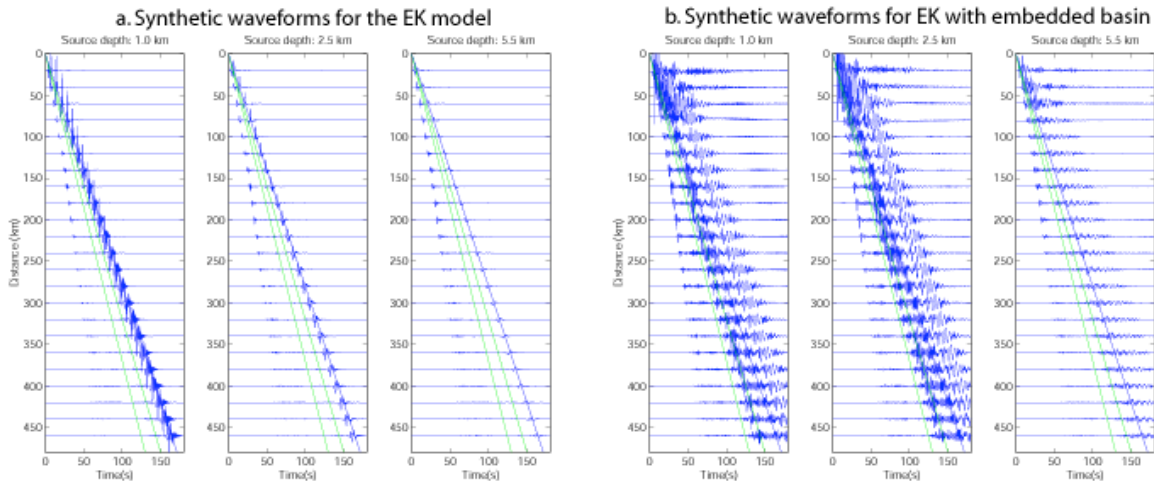


Figure 5. Synthetic seismograms generated for the EK model and a modified EK model with an embedded basin. Times corresponding to 3.7 km/s and 3.2 km/s are marked in green, 2.8 km/s in blue.

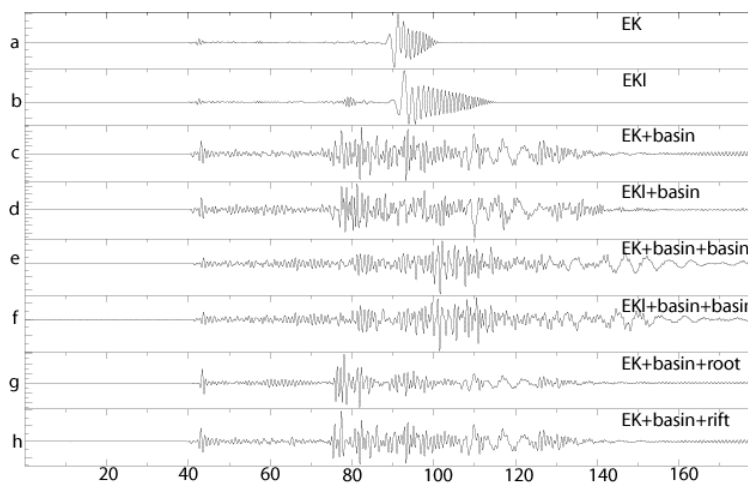


Figure 6. Vertical component synthetic seismograms generated for a range of models based on EK, recorded at 260 km from the source, filtered between 0.01 and 1.5 Hz.

**Effect of source depth with an embedded basin.** There was little difference in the arrival time characteristics generated for sources at different depths in the basin. However, the amplitude of the primary arrivals and, more drastically, of the *Lg* were increased significantly (Figure 5b) for sources at shallower depths within the basin. Adding more complexity to this structure had little contribution to the source-depth effect.

**Effect of structure on generation and propagation.** The large amplitude *Lg* generated for sources in the basin propagates beyond the extent of the low velocity structure (in the models used to create Figure 5b, the basin extends to 80 km from the source). There was little difference in the *Lg* window between waveforms generated for the simple EK model with embedded basin (Figure 6c) and the EK model with an uppermost low velocity layer and embedded basin (Figure 6d); however, in the *Rg* window low frequencies are delayed. When the source is placed underneath the basin the amplitudes of the surface waves are greatly reduced compared to those generated for shallow sources (Figure 5b); in this case the presence of a low velocity uppermost layer has a more notable effect. A crustal thickening next to the basin (Figure 6g) shifts more energy into the earlier part of the *Lg* window while the presence of a second basin below the receiver has the opposite effect (Figures 6e and 6f). Thinning of the crust (Figure 6h) below the basin has little effect on generation and propagation. We will continue modeling the effects of common tectonic structures on the generation and propagation of *Rg* and *Lg*.

**GFM2D Modeling of the Regional *Lg* from the DOB Explosions.** We performed a final test of the capabilities of GFM2D by modeling the *Lg* generated from the DOB explosions at regional distances. Our initial model for this evaluation was the Eastern Kazakhstan (EK) model of Priestley *et al.* (1988), which was used in the Xie and Lay (1994) paper on *S*-wave generation using finite-difference modeling. The model was converted to GFM2D format and is 514 km long and 171 km deep, with a grid spacing of 0.5 km. It should be noted that the EK model has a *P*-wave velocity in the upper crust of 5.05 km/s, which was greater than the mantle-lid velocity of 4.57 km/s. Some authors (e.g., Frankel, 1989) have noted that for these *P*- and *S*-wave velocities, it is impossible to trap *S*-waves in the crust to form the *Lg* phase. Our synthetics from the EK model agree with this interpretation, as the energy in the *Lg* group velocity window was composed of very weak *S\** arrivals.

To provide a comparison with the EK model, we then generated synthetics for the Shagan+EK model. The local *Rg* recorded at the Shagan test site for these explosions suggests that the near-surface *P*-wave velocities are less than 4.8 km/sec, which is the mantle-lid velocity in the EK model. Thus, in accordance with Frankel (1989) and Xie and Lay (1994), the Shagan+EK model should be suitable for trapping shear-waves in the crust with the appropriate *Lg* group velocity. The GFM2D synthetics in Figure 7 show significant energy in the *Lg* window for this model. For a grid spacing of 0.5 km, the *P*-waves are accurate up to ~6 Hz, the *S*-waves are accurate up to ~3 Hz, and the *Rg* is accurate to between 1 and 2 Hz. Figure 7 shows a comparison of both model runs for a single station at 288 km. Clearly, the Shagan+EK model traps more energy in the form of surface *P* to *S* conversions and subsequent multiple reflections than the EK model. The Shagan+EK model also spreads out the surface waves as a result of the low-velocity shallow layers; however, if intrinsic attenuation were considered in the GFM2D runs, these later-arriving higher-frequency surface waves would most likely be attenuated below the noise level.

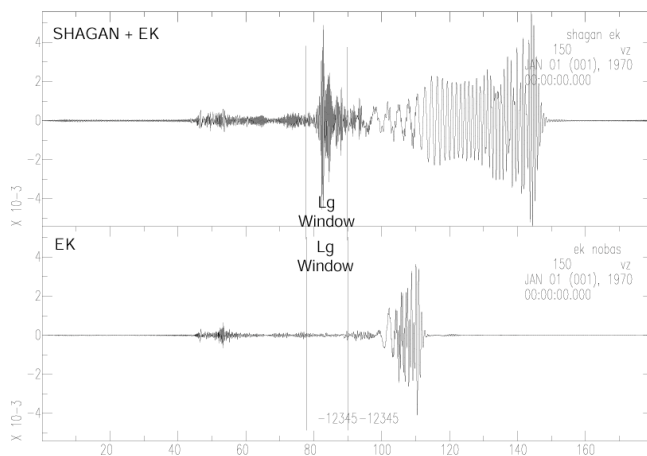


**Figure 7. Comparison of SHAGAN+EK synthetics vs. EK only synthetics at X=288 km.**

We used the Shagan+EK velocity model to synthesize the seismograms for the DOB explosions at station MAK. Explosion point sources were buried at 50 m, 300 m, and 550 m within the model. Then, GFM2D was employed to generate 200 seconds of data recorded at stations that were 421 km (MAK) from the sources. The synthetic data were then convolved with a Mueller-Murphy source (Mueller and Murphy, 1971) determined using the depth of each shot and the Shagan+EK model. A comparison of observed and synthetic  $Lg$  spectra is presented in Figure 8. Between 0.7-3 Hz, the relative  $Lg$  spectral amplitudes for the observed and synthetic data, as normalized to the 50 m explosion at 1 Hz, are similar, even when we consider the fact that the shallow explosion created a large crater. We observe that the shapes of the spectra have disparities. First, below 0.7 Hz, the observed data contains microseismic noise that boosts the amplitudes while the synthetic data is noiseless at these frequencies. The differences between the synthetic spectra at frequencies below 0.7 Hz are related to the addition of the Mueller-Murphy source component. Second, the synthetic spectral amplitudes decrease at a greater rate than the observed spectra between 1-3 Hz, possibly due to the large spectral null around 2.3 Hz. We see smaller nulls in the observed spectra for the DOB explosion followed by an increase in amplitudes. These results suggest that a significant proportion of the  $Lg$  amplitudes observed at station MAK may be explained as the effect that different source depths have on the amplitudes of the  $P$  to  $S$  surface reflection above the source. The remaining differences may be related to the effects of the CLVD source and near-source scattering of  $Rg$  to  $S$ . Figure 9 presents the  $Pg/Lg$  amplitude ratios for the synthetic and observed MAK data. For the observed data between 1 and 3 Hz, the 550 m explosion had the largest  $Pg/Lg$  ratio, followed by the 50 m explosion and the 300 m explosion. We observe the same order for the synthetic data, however there is a significant offset, possibly due to significant  $Rg$ -to- $P$  scattering in the observed data (Gupta *et al.*, 1991).

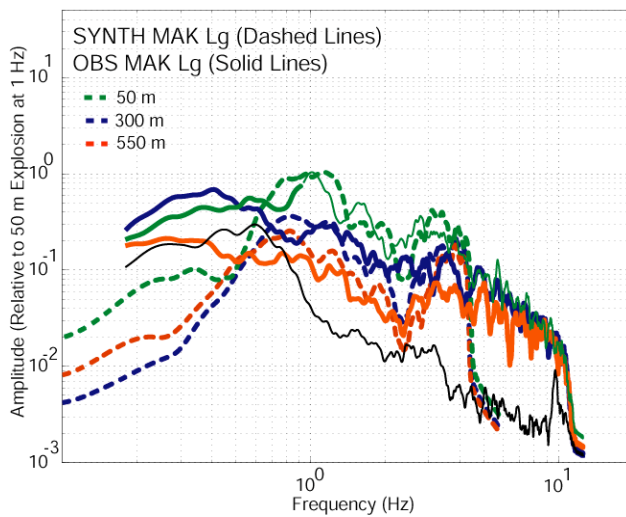


**Figure 8. Displacement spectra for observed  $Lg$  (solid lines) and synthetic  $Lg$  for station MAK for the 50 m, 300 m, and 550 m DOB explosions at the Shagan Test Site. Also shown is the noise level at MAK (solid black line) for the same day that the 50 m explosion was detonated. The data have been normalized to the 1 Hz spectral amplitude of the 50 m explosion.**

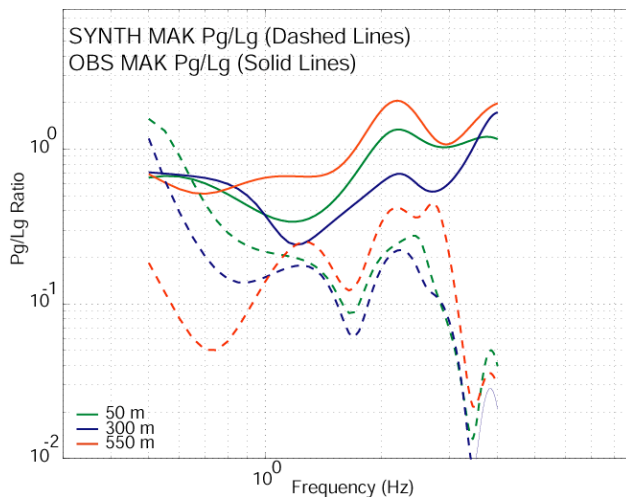


**Figure 9.  $Pg/Lg$  ratios (observed=solid; synth=dashed) for the MAK DOB data.**

## **CONCLUSIONS AND RECOMMENDATIONS**

It is critical that a physical model for the genesis of regional  $S$  waves be well understood for underground explosions. One possible mechanism of generating  $S$  waves is by  $Rg$ -to- $S$  scattering in which  $Rg$  waves are excited by a spatially-distributed source composed of the explosion and an inverted conical zone undergoing catastrophic shear failure above the dilatational point source. This conical source is equivalent to a compensated linear vector dipole (CLVD), which has been used to explain the frequency content of  $Lg$  spectra and spectral ratio observations for nuclear explosions (Patton and Taylor, 1995; Gupta *et al*, 1997). Observations of the  $Rg$  amplitude and phase spectra presented in this paper cannot be modeled adequately by a pure explosion monopole source for any DOB explosion, including the overburied 550 m explosion with sDOB of 1400. Thus, we are now examining whether a linear superposition of a monopole and a CLVD source can be used to improve the fit to the observed spectra.

We have observed that GFM modeling can provide improved understanding of the genesis of explosion-generated  $S$ -waves using 2D and 3D simulations. We have completed 3D simulations of  $Lg$  and  $Rg$  generation in 3D structures for NIL, and we have used the modeling to estimate the velocities for these phases. Additionally, we have used 2D GFM simulations to examine the effects of basins, crustal roots, and crustal thinning on the genesis of  $Lg$  and  $Rg$ . GFM simulations showed the EK model derived synthetics do not exhibit shear waves (e.g.,  $Sn$  and  $Lg$ ) similar to those observed from the Shagan Test Site DOB explosions; however, by attaching the shallow velocity structure determined from  $Rg$  inversions at the Shagan Test Site to the EK model, large amplitude shear-wave arrivals (both  $Sn$  and  $Lg$ ) can be trapped within the crust. The arrivals in the  $Lg$  window consist of multiple-reflected  $S$ -waves resulting from the initial conversion of  $P$  to  $S$  at the free surface above the source. Synthetics generated by convolving GFM2D Green's functions with a Mueller-Murphy source at different depths can account for as much as 80% of the observed amplitude differences in the 1-3 Hz bandwidth at station MAK; however, differences in the shape of the spectra may result from the fact that the explosions were not pure monopoles. The  $Pg/Lg$  ratios observed from the MAK data are consistent with the synthetic data in terms of order as a function of DOB; however, the relative synthetic  $Pg$  amplitudes are smaller than the observed amplitudes.

## **REFERENCES**

- Bassin, C., G. Laske, and G. Masters (2000), Current limits of resolution for surface wave tomography in North America, *EOS Trans AGU*, **81**, F897.
- Bonner, J.L., D.C. Pearson W.S. Phillips, and S.R. Taylor (2001), Shallow velocity structure at the Shagan Test Site in Kazakhstan, *Pure and Applied Geophysics*, 158, 2017-2039.
- Denny, M.D. and L.R. Johnson (1991), The explosion seismic source function: models and scaling laws reviewed, in Taylor, S.R., H.J. Patton, and P.G. Richards, Eds. *Explosion Source Phenomenology*, American Geophysical Union Monograph 65, 1-24.
- Frankel, A. (1989), Effects of source depth and crustal structure on the spectra of regional phases determined from synthetic seismograms, *DARPA/AFTAC Annual Seismic Research Review* FY 89, Air Force Technical Applications Center, Scientific Report, 97-118.
- Gupta, I. N., W. Chan, and R. Wagner (1992), A comparison of regional phases from underground nuclear explosions at East Kazakh and Nevada Test Sites, *Bull. Seism. Soc. Am.* **82**, 352-382.
- Gupta, I.N., T.R. Zhang, and R.A. Wagner (1997), Low frequency  $Lg$  from NTS and Kazakh nuclear explosions-observations and interpretation, *Bull. Seism. Soc. Am.* **87**, 1115-1125.
- Meyers, S.C., W. R. Walter, K. Mayeda, and L. Glenn (1999), Observation in support of  $Rg$  scattering as a source of explosion  $S$  waves: regional and local recordings of the 1997 Kazakhstan depth of burial experiment, *Bull. Seism. Soc. Am.* **89**, 544-549.
- Mueller, R.A., and J.R. Murphy (1971), Seismic characteristics of underground nuclear detonations, *Bull. Seism. Soc. Am.*, **61**, 1675-1692.
- Orrey, J. L., C. B. Archambeau and G. A. Frazier (2003), Complete Seismic Wave Field Synthesis with a Pseudospectral Method: The Generalized Fourier Method, revised manuscript submitted to *Geophys. J. Int.*
- Patton, H.J., and S. R. Taylor (1995), Analysis of  $Lg$  spectral ratios from NTS explosions: implications for the source mechanisms of spall and the generation of  $Lg$  waves, *Bull. Seism. Soc. Am.* **85**, 220-236.
- Priestley, K. F., G. Zandt, and G. E. Randall (1988), Crustal structure in Eastern Kazakh, USSR from teleseismic receiver functions, *Geophys. Res. Lett.*, **15**, 613-616.
- Xie, X. and T. Lay (1994). The excitation of  $Lg$  waves by explosions: a finite-difference investigation, *Bull. Seism. Soc. Am.*, **84**, 324-342.